Available online at www.sciencedirect.com
ScienceDirect
Diamond & Related Materials 16 (2007) 1958–1966
DIAMOND AND RELATED MATERIALS
www.elsevier.com/locate/diamond

Parametric study of atmospheric-pressure single-walled carbon nanotubes growth by ferrocene–ethanol mist CVD

S. Chaisitsak [a,*], J. Nukeaw [b], A. Tuantranont [c]

[a] Department of Electronics, Faculty of Engineering, King Mongkut's Institute of Technology Ladkrabang, Bangkok 10520, Thailand
[b] Faculty of Science, King Mongkut's Institute of Technology Ladkrabang, Bangkok 10520, Thailand
[c] National Electronics and Computer Technology Center, Pathumthani 12120, Thailand

Received 20 December 2006; received in revised form 20 August 2007; accepted 12 September 2007
Available online 22 September 2007

Abstract

Uniform web-like films consisting single-walled carbon nanotubes (SWCNTs) were deposited on a silicon substrate using the chemical vapor deposition (CVD) of ferrocene–ethanol mist at atmospheric pressure (~1 atm). The tiny mist was generated using a high-frequency ultrasonic vibration. The effects of various parameters including deposition position in the reactor, temperature, ferrocene/ethanol ratio, flow rate of carrier gas (argon), and deposition time on the formation of SWCNTs was investigated using high-resolution scanning electron microscopy, transmission electron microscopy and Raman spectroscopy. The worm region outside the furnace was found to be a suitable position for the formation of SWCNT films. The furnace temperature and the flow rate of carrier gas were found to determine the diameter and crystallinity of nanotube. The ferrocene concentration in ethanol strongly influenced the amount of impurity particles in the material. Moreover, the intensity of metallic tail in D-band was found to decrease with increasing the flow rate, showing a possibility of the formation of semiconducting SWCNTs. Results of this study can be used to improve understanding of the growth of SWCNTs by floating catalyst CVD of alcohol mist.

Keywords: Carbon nanotubes; Chemical vapor deposition (CVD)

1. Introduction

Since 1991, carbon nanotubes (CNTs) [1] have attracted much attention as a new material due to their outstanding mechanical and electronic properties. In general, structure of multi-walled CNTs (MWCNTs) has more defects than single-walled CNTs (SWCNTs). SWCNTs can be conducting or semiconducting wires depending on the tube diameter and chirality, and can be twisted and bent without breaking [2]. Among the variety of synthesis techniques for SWCNTs, the chemical vapor deposition (CVD) [2] is the most suitable method for industrial-scale production, because of its upward scalability, low cost and low deposition temperature.

The CVD offers the benefit of the use of solid, liquid and gaseous carbon sources. Maruyama et al. were the first to succeed in synthesis of high-purity SWCNTs from liquid alcohols (methyl, ethyl) using a thermal CVD over Fe–Co catalysts supported on zeolite [3]. Subsequently, Shinohara's group also demonstrated the synthesis of high-purity SWCNTs under atmospheric pressure on catalytic powders using an alcohol CVD method [4]. It is believed that an OH radical from oxygenated organic vapor can eliminate amorphous carbons in the deposition [3] and purification processes of SWCNTs [5]. Using the floating catalyst approach, Windle's group used ethanol solutions in the presence of ferrocene, sulphur and hydrogen at 1200 °C, to continuously synthesize SWCNT ropes [6]. More recently, Lupo et al. reported the pyrolytic synthesis of web-like SWCNTs in a heated flow of ferrocene–ethanol solutions in the absence of sulphur and hydrogen at 800–950 °C [7].

Here, we presented the deposition of SWCNT films by an alternative CVD using ferrocene–ethanol mist under atmospheric pressure. In this method, the mist of ferrocene and ethanol, generated by a high-frequency ultrasonic atomizer, were used as a catalyst precursor and a carbon source,

* Corresponding author. Tel.: +66 2 326 4222; fax: +66 2 739 2398.
E-mail address: kcsutich@kmitl.ac.th (S. Chaisitsak).

0925-9635/$ - see front matter © 2007 Elsevier B.V. All rights reserved.
doi:10.1016/j.diamond.2007.09.013

respectively. The pyrolysis process using the mist of liquid source is an effective technique to grow spherical and homogeneous particles compared to any other processes [8]. Thus, modifying the ferrocene–ethanol in a mist form [7,9–13] makes it possible to continuous production of uniform SWCNT films, since it is a continuous process of both catalyst particle formation and nanotube growth. However, little information is available on the influence of growth parameters on SWCNT growth [7,10,12,13]. In this paper, the effects of various growth parameters (deposition position in the reactor, furnace temperature, ferrocene concentration in ethanol solution, flow rate of carrier gas and deposition time) on the formation of nanotubes were investigated using scanning electron microscopy (SEM), transmission electron microscopy (TEM) and Raman spectroscopy. The results of this study could be useful for mass-production of SWCNT film, since our modified CVD is simple, low cost for maintenance and does not require vacuum or hydrogen containing system.

2. Experimental

Our CVD system was based on the catalytic decomposition of liquid hydrocarbon by atomizing solutions of both the hydrocarbon source and the catalytic precursor. Ethanol (C_2H_5OH, 99.8%) and ferrocene ($Fe(C_5H_5)_2$, 98%) were used as a carbon source and a catalytic precursor, respectively. The growth system consisted of a mist-generating unit, a mist-carrying unit, a heating unit and a reaction unit, as illustrated in Fig. 1(a). A horizontal tubular furnace of ~25 cm long and a quartz reactor of ~50 cm long and 1 cm outer diameter were used. The processes for aqueous ferrocene–ethanol solution are as follows: 0.1–3 wt.% of ferrocene relative to ethanol was dissolved in ethanol; subsequently the solution was ultrasonically stirred for 30 min, giving a clear orange/brown solution; finally the solution was transferred into the container attached to a mist generator. The mist generator was based on an electrical ultrasonic atomizer (~1.7 MHz, 20–30 W). The droplet average diameter was estimated to be about ~2.4 μm using the relation $D_d = 0.34(8\pi\gamma/\rho f^2)^{1/3}$ [14], where D_d is the droplet diameter, γ is the solution surface tension (21.55×10^{-3} N/m for pure ethanol), ρ is the solution density (789 kg/m^3 for pure ethanol), and f is the applied ultrasonic frequency (~1.7 MHz). Silicon substrates were loaded into the reactor at the middle zone and also at the outside zone of the furnace to collect the deposited CNTs. After connecting all equipment (Fig. 1(a)), argon (99.99%) 1.0–2.0 L/min was fed into the system for 10 min to eliminate oxygen from the system. Then, the furnace was heated to the setting temperature (650–800 °C) in 30 min. After furnace temperature was stable, the atomizer was turned on, creating a small droplet of ferrocene–ethanol. In order to avoid the condensation of mist prior to the pyrolysis process, the distance between the solution container and the quartz reactor was minimized. The consumption rate of the solution was ~0.7 g/min, determined by weighting the container. The argon flow rate for blowing the mist into the reactor was set in the range of 0.5–3.0 L/min. After 1–30 min of deposition time, the atomizer was turned down and the reactor warmed down gradually to room temperature under argon atmosphere. All experiments were performed at atmospheric pressure. The resulting CNTs grew both on the silicon substrates and on the inner surface of quartz reactor as a black mat-like film that could be easily scraped off.

The characterization of as-grown CNTs on Si substrates was performed by field-emission scanning electron microscopy (SEM), transmission electron microscopy (TEM) as well as energy-dispersive X-ray (EDX). Raman spectroscopic measurements were also carried out at room temperature in the range of 150–2000 cm^{-1} with a resolution of 1.7 cm^{-1} using Ar laser (514.5 nm excitation). Most of the spectra in this work were averaged over three different positions on the sample.

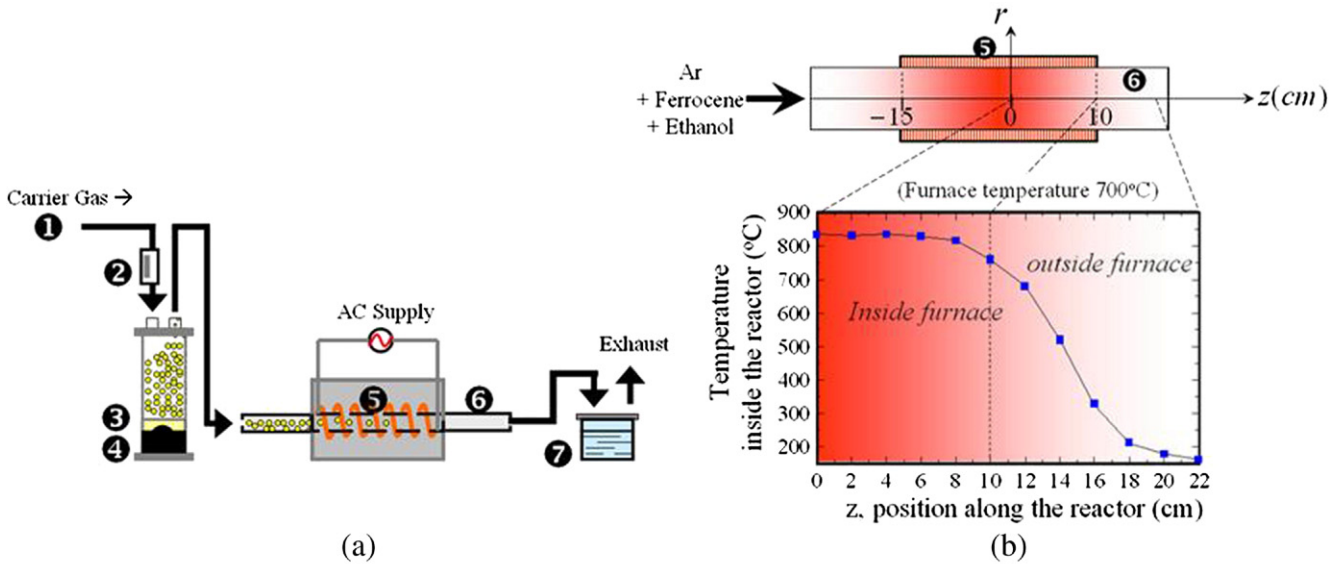

Fig. 1. (a) Schematic diagram of the floating catalyst CVD using ferrocene–ethanol mist; ❶ carrier gas (argon) entrance ❷ flow controller ❸ ferrocene–ethanol container ❹ atomizer ❺ furnace ❻ quartz reactor ❼ water trap. (b) Temperature profile inside the reactor when the furnace temperature was set to 700 °C.

3. Results and discussion

3.1. Effect of the deposition position in the reactor

In our CVD system, the thermocouple to control furnace temperature was set at the middle of furnace outside the quartz reactor. In order to measure the temperature inside the reactor during the deposition process, a thermocouple (type K) was inserted from the open-end side of the reactor. Fig. 1(b) shows the reactor temperature profile measured for 700 °C furnace temperature. In this case, the reactor temperature at the center was as high as ~800 °C and relatively uniform over the region of furnace zone. Typically, the temperature inside the reactor was usually higher than the setting temperature by 20–100 °C, depending on the growth parameters. However, at the outsize of furnace zone (z>10 cm) the reactor temperature reduced significantly, as shown in Fig. 1(b). At 6 cm away from the exit of furnace (z=16 cm) the temperature was only ~300 °C. It is important to note that the formation of CNTs not only occur at the inside of furnace (hot region) but also at the outside of furnace (worm region). The wall surface of quartz tube turned to dark back after about 5–10 min of the reaction time in the direction of carrier gas flow, depending on the flow rate and ferrocene concentration. To investigate the effect of deposition position in the reactor on the formation of CNTs, the morphology and Raman spectra data were taken at different points along the reactor axis.

Fig. 2 shows SEM images of CNT films deposited at different positions along the reactor axis (z-axis as illustrated in Fig. 1(b)). The deposition conditions were 700 °C furnace temperature, 1.5 wt.% ferrocene/ethanol ratio, 0.5 L/min Ar flow rate and 15 min deposition time. Clearly, these SEM images show a significant position-dependent morphological change. For the film deposited inside the furnace (hot region, Fig. 2(a)), large diameter filaments (diameter ≈ 10–50 nm) were observed with a coexistence of helical fibers and large particles. Although further increase in furnace temperature could enhance the amount of narrow tubes in the films, the films mainly consisted of large tubes (diameter > 10 nm). Thus the hot region is not a suitable position toward SWCNTs. On the contrary, the films deposited outside the furnace (warm region, Fig. 2(b) and (c)) showed a larger number of narrow tubes (diameter < 10 nm). A similar result of web-like material obtained outside the furnace region has been observed by several authors for a CVD of ferrocene [7,13,15]. However, no work has been done on the effect of the deposition position outside the furnace on the property of formed CNTs. At this point, we confirmed that all of the films deposited outside the furnace showed the same morphology, as shown in Fig. 2(b–c). Moreover, all films consisted of SWCNT bundles with a tube diameter of ~1 nm, evaluated from Raman scattering data and TEM observation. It should be noted that the blackness of the obtained films reduced as the distance away from the exit of furnace increased, indicating a decrease in film thickness. However, the actual thickness did not measure in this study. Furthermore, it can be seen that all films deposited outside the furnace usually attached with catalyst particles, identified as iron/iron oxide (using EDX), regardless of deposition position (Fig. 2 (b–c)). However, the amount of these particles could be reduced by decreasing the ferrocene concentration in the ethanol solution, as will be described later.

Raman spectroscopy technique [16] was used to characterize diameter distribution, crystallinity and impurity of the CNTs. Fig. 3(a) and (b) shows the Raman spectra in the low-frequency

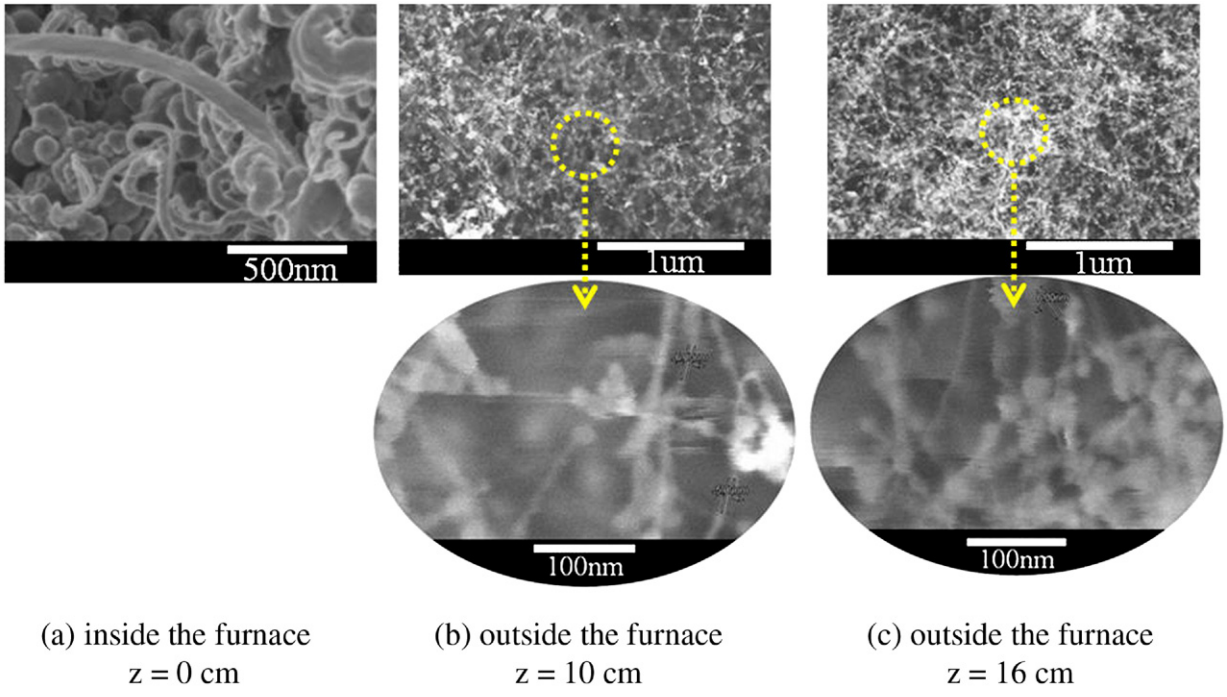

Fig. 2. SEM images of CNT films deposited at different positions along the reactor axis (z-axis as illustrated in Fig. 1(b)). (a) Film deposited inside the furnace (hot region): at the middle zone of furnace, z=0 cm; filaments with a large diameter (10–50 nm) were observed with a coexistence of large particles. (b and c) Films deposited outside the furnace (worm region): (b) at the end of furnace, z=10 cm and (c) at z=16 cm. Both samples had a larger number of long and narrow CNTs.

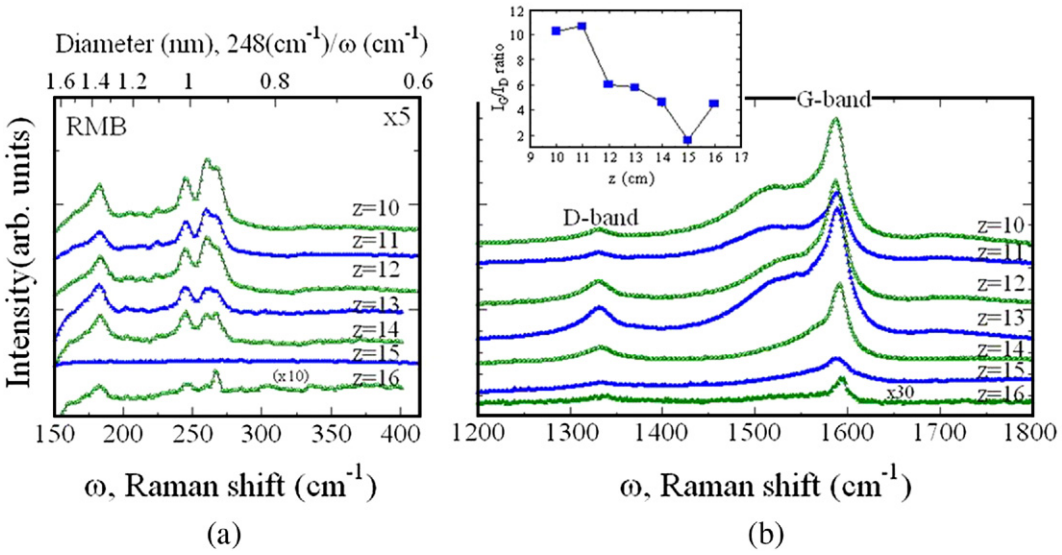

Fig. 3. (a) Raman spectra in the RBM region of CNT films deposited outside the furnace as a function of z-position (see definition in Fig. 1(b)). Nanotube diameter (d_t) was determined by using $d_t = 248/\omega_{RBM}$. (b) Raman spectra in high-frequency region of the samples in (a) showing G-band (1530–1590 cm^{-1}) and D-band (1330 cm^{-1}). Inset in (b) shows the ratio of integrated intensities of the D-band peak to the G-band peak (I_G/I_D) of all the samples. Growth parameters; furnace temperature: 700 °C, argon flow rate: 0.5 L/min, ferrocene/ethanol ratio: 1.5 wt.%, 15 min.

region (150–400 cm^{-1}) and high-frequency region (1200–1800 cm^{-1}), respectively, of the CNTs deposited outside the furnace at different z-position. It can be seen that the Raman shifts in low-frequency region were nearly independent of the position of the samples. The Raman spectra of all samples showed multiple radial breathing mode (RBM) peaks between 180 cm^{-1} and 270 cm^{-1}. The corresponding diameters of SWCNTs were in the range of 0.9–1.4 nm, using the empirical relation $\omega_{RBM} = 248/d_t$, where d_t and ω_{RBM} are the tube diameter (nm) and the Raman shift (cm^{-1}), respectively [16]. Those estimations are in agreement with the diameters obtained from TEM observation.

In Fig. 3(b), the broad band at 1330 cm^{-1} is ascribed to as the D-band due to various forms of disordered or nanocrystalline carbons. The intense G-band at 1530–1590 cm^{-1} is assigned to the tangential mode of the highly ordered graphite. A clearly observed multiple-splitting of the G-band also provides a reliable indication of a presence of SWCNTs within the samples [16]. Inset in Fig. 3(b) shows the relative intensities of G-band to D-band (i.e. I_G/I_D) used as a purity/crystallinity index to assess the quality of SWCNTs [17]. All of the samples in Fig. 3 had an I_G/I_D value much greater than unity. The I_G/I_D of the samples deposited near the exit of furnace ($z = 10$–11 cm, reactor temperature: ~700 °C) was relatively high (>10), indicating a high crystallinity in the present samples. On the other hand, the I_G/I_D value decreased as increasing the distance away from the exit of furnace. The I_G/I_D value decreased to ~4 when the samples were placed more than 4 cm away from the exit of furnace ($z > 14$ cm, reactor temperature: <500 °C). For the higher furnace temperature, however, the less change in I_G/I_D value could be observed. At this point, we suggest that the incomplete decomposition of ferrocene and/or ethanol in the warm region when compared to the hot region could occur, resulting in the formation of carbon product. This would lead to the high intensity of D-band and subsequently lower the I_G/I_D value, as seen in the samples placed at $z > 14$ cm.

3.2. Typical SWCNT films

Using the present method, as described earlier, the SWCNT films can be obtained outside the furnace (worm region) even at low temperature areas. Therefore, this SWCNT material was used for this study. By controlling the reaction parameters, as will be described in the next sections, the deposition of high-crystallinity SWCNT films can be realized.

Fig. 4(a–b) and (c) shows typical SEM and TEM images of the SWCNT film deposited outside of the furnace under an optimal condition. Using our experimental set-up, raw materials produced at a rate of about 0.3 mg/min. The I_G/I_D value of the material was about 9, which is comparable to the previous reports of SWCNTs by a CVD using spraying ferrocene/ethanol [7,10]. Compared to those works, however, the obtained material had a more uniform SWCNT film, as shown in Fig. 4(a–b). It was found that the SWCNTs deposited by ferrocene–ethanol method tend to grow in a bundle or a rope rather than in an individual tube, as demonstrated in Fig. 4(c). Moreover, as mentioned before, the SWCNT bundle usually adhered with spherical particles (diameter in 4–30 nm range). However, the catalyst particles that resided in the hollow structure of SWCNTs were not observed. EDX analysis in Fig. 4(e) indicated that these particles consisted of iron, oxygen and carbon; the copper and silicon signals were attributed to a copper TEM grid and a silicon substrate. The form of these particles is unclear and could either be Fe_3C or iron oxide (Fe_2O_3, Fe_3O_4), since these kinds of compounds have been found in CNTs grown by a CVD of ferrocene [11]. It should be noted that these particles usually had larger diameter than that of tubes and were encapsulated by thin graphitic layers as shown in Fig. 4(d). Previous study performed by Hou et al. [15] indicated that the carbon-enclosed iron particles could be formed by the self-decomposition of ferrocene at 600–700 °C.

We expect that these catalysts become inactive, due to their large particle size.

We believe that the achievement in the deposition of SWCNTs with high crystallinity and less undesirable particle could be due to the greater decomposition effect of ferrocene/ethanol solution under tiny mist atmosphere together with the etching effect of OH radical from ethanol under high temperatures [3]. However, the growth process of CNTs was not clear and the growth mechanism needs further research.

3.3. Effect of the furnace temperature

In the second series of experiments, the furnace temperature was varied from 650 °C to 800 °C, while the argon flow rate, ferrocene/ethanol ratio and growth time were kept constant at 1.0 L/min, 0.1 wt.% and 15 min, respectively. Here, SWCNT films were deposited on Si substrates at the end of furnace (z=10 cm).

Fig. 5(a) shows SEM images of the CNT films grown outside the furnace at different furnace temperatures. Fig. 5(b) and (c) shows the corresponding Raman spectra in RBM frequency region and high-frequency region, respectively. As shown in Fig. 5(a), the formation of narrow tubes could be observed even at a low temperature of 650 °C when compared to the previous works using different carbon precursors [9,11,15,18,19]. However, at the temperature 650 °C and below the coexistence with large diameter tubes was observed, and tended to disappear with increasing the furnace temperature. The deposition of SWCNT films at low temperatures could be possible due to the low decomposition temperature of ferrocene (~400 °C) [20] together with the etching effect of OH radical from ethanol precursor [3].

An existence of SWCNTs for all furnace temperatures was also confirmed by the appearance of narrow RBM peaks in Raman spectra, as plotted in Fig. 5(b). It is found that the RBM peaks shifted toward lower frequencies with increasing the furnace temperature, indicating that the diameter of CNTs became larger. This observed temperature dependence of the tube diameter is similar to that reported by Singh et al. [12] in a ferrocene/toluene-based CVD, Zhang et al. [19] in a ferrocene/xylene-based CVD and Moisala et al. in a ferrocene/CO CVD [21]. This could be assumed that under the high temperature the frequency of metal particles collision increases [22], resulting in an increase in the particle diameter. As a consequence, the diameter of CNTs becomes larger.

As presented in Fig. 5(c), the I_G/I_D value increased with increasing the furnace temperature, indicating an increase in crystallinity of the films. This result is in agreement with data presented in a previous paper [3] using alcohol CVD over a Fe/Co catalyst. This crystallinity enhancement is possibly due to the reduction of carbon products decomposed from ferrocene/alcohol at a high temperature. In this experiment, the film deposited at 800 °C exhibited the highest I_G/I_D value of about 3.2. As will be described later, however, by optimizing the ferrocene/ethanol ratio, the I_G/I_D value can be increased.

3.4. Effect of the ferrocene/ethanol ratio

It is believed that the size of catalyst particles controls the diameter of nanotubes formed. In the third series of experiments, the influence of ferrocene concentration in ethanol solution (ferrocene/ethanol ratio) on the quality of SWCNTs was investigated. Here, the ferrocene/ethanol ratio was varied in the range of 0.1 wt.%–3.0 wt.%, while the furnace temperature, argon

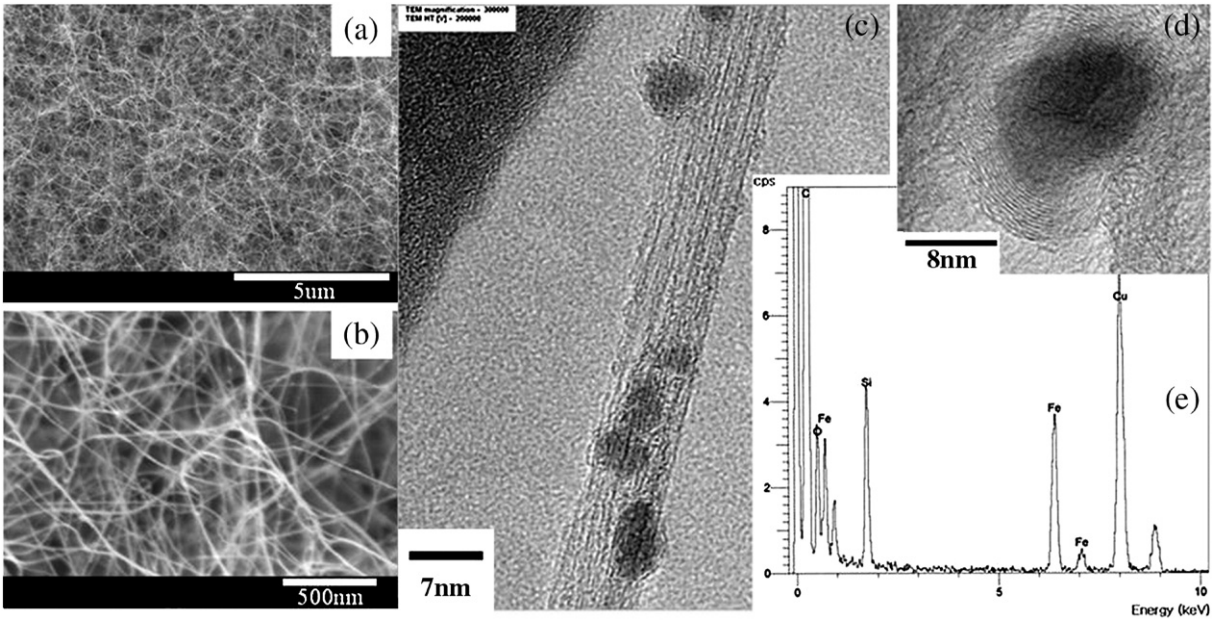

Fig. 4. Typical images and spectrum of a CNT film deposited outside of furnace (position: z=10 cm, furnace temperature: 700 °C, argon flow rate: 1.0 L/min, ferrocene/ethanol ratio: 1.0 wt.%, 15 min); (a) low magnification SEM image, showing uniform web-like CNTs. (b) Higher magnification SEM image of (a), confirming the narrow-diameter tubes. (c) TEM image of a bundle of SWCNTs with catalyst particles. (d) TEM image of a graphite-coated particle. (e) EDX spectrum of the particle in (d), indicating the existence of iron, carbon and oxygen.

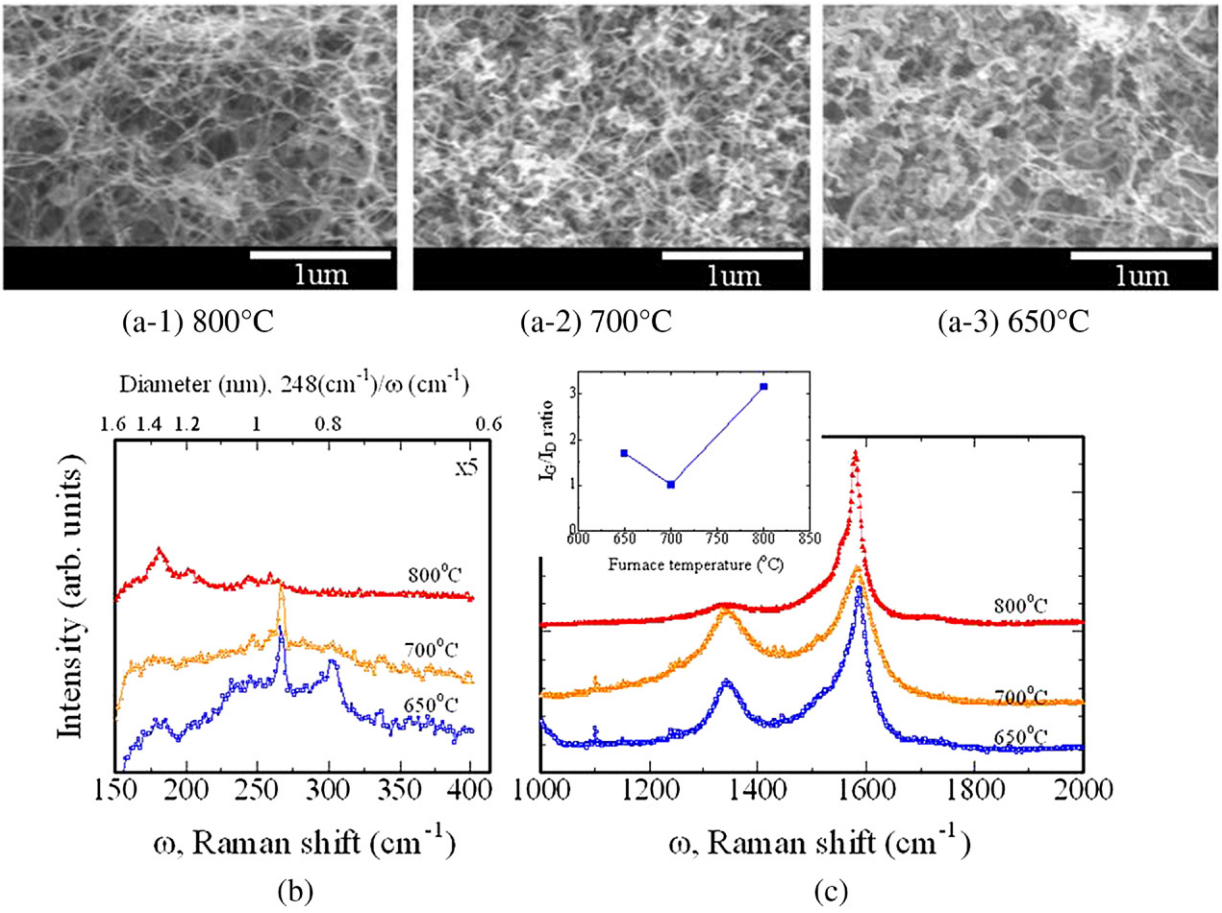

Fig. 5. (a) SEM images of CNTs deposited outside the furnace as a function of furnace temperature. (b and c) Corresponding Raman spectra in low-frequency region and high-frequency region, respectively. Inset in (b) shows the I_G/I_D value as a function of furnace temperature. Growth parameters; argon flow rate: 1.0 L/min, ferrocene/ethanol ratio: 0.1 wt.%, position: $z=10$ cm, 15 min.

flow rate and growth time were kept constant at 700 °C, 1.0 L/min and 15 min, respectively.

Fig. 6(a) shows SEM images of the CNT films deposited at the different ferrocene/ethanol ratios; (a-1) 3.0 wt.%, (a-2) 1.0 wt.% and (a-3) 0.1 wt.%. These SEM results revealed that the density of SWCNTs and the number of undesirable products in the films could be optimized by varying the ferrocene concentration. Using a low concentration, few narrow-size tubes with a large formation of a-C were observed as shown in Fig. 6(a-3) (0.1 wt.%). One possible explanation is that the solution is so dilute that less catalyst particles, and subsequently, less CNTs grow. However, the number of narrow-size tubes could be increased by increasing the ferrocene/ethanol ratio. In contrast to the low concentration case, a too high concentration would result a large number of particle impurities, as shown in Fig. 6(a-1) (3.0 wt.%). Moreover, a large amount of a-C could be observed as a low I_G/I_D value, since a large number of catalyst particles can not nucleate CNTs. A similar relation between the undesirable products (a-C and metallic impurity) and the ferrocene concentration was previously reported by Kumar et al. using a ferrocene–camphor-based CVD [18] This finding implies that the dosage amount of ferrocene in ethanol solution, and thus, the production rate of CNTs are limited. According to our results, the optimal concentration was 1.0–1.5 wt.% for our deposition system, to get less a-C and particle impurities in the resulting CNT films.

Fig. 6(b) and (c) shows the Raman spectra of CNT films as a function of ferrocene/ethanol ratio. For every case, RBM peaks were clearly observed. It was found that the RBM of the films deposited at a low ferrocene/ethanol ratio (e.g. 0.1–0.5 wt.%) usually showed a narrow peak, indicating a narrow distribution of tube diameter in the material. On the other hand, for the films deposited at a high ferrocene/ethanol ratio (e.g. 1.0–3.0 wt%), multiple RBM peaks were observed, resulting in an existence of SWCNTs with various tube diameters. The decrease in diameter distribution by reducing the catalyst concentration has been reported for SWCNTs/MWCNTs produced by an injection of ferrocene–toluene system [12] and for SWCNTs synthesized by alcohol CVD [23].

Singh et al. and Hou et al. reported that the larger CNTs would form with increasing the ferrocene concentration in a ferrocene–toluene [12] or ferrocene–anthrracene [15] system. They believed that the aggregation of catalyst atoms increases as an increasing of ferrocene concentration, resulting in the formations of large particles and large CNTs. In our case, however, we found that the tube diameter was not clearly related to the ferrocene concentration for the studied range, as shown in the Raman results in Fig. 6 (b). We believed that the difference in obtained results may be related to the difference in feeding method of catalysts into the reactor. Compared to the spraying [12] or evaporating [15]

methods used in their works, in our growth system the dilute catalyst solution was atomized by a high-frequency atomizer and then carried into the reactor in the form of tiny droplets. This would lead to the formation of tiny catalyst particles. To clarify this, however, further investigation on the effect of droplet size on the formations of catalyst and nanotube is required.

The ferrocene/ethanol ratio was also a critical factor to deposit high-crystallinity SWCNT films in our experiments, as shown in Fig. 6(c). SWCNTs with highly ordered graphitic structures were obtained at the ferrocene/ethanol ratio of in a range of 1–1.5 wt.%. The I_G/I_D value decreased both above and below this range. At high concentrations, as mentioned before, an increasing amount of inactive catalyst might become significant. This would result in a high intensity of D-band, and subsequently, lower the I_G/I_D value as found in the sample prepared at 3.0 wt.%. On the other hand, the films deposited at low concentrations (e.g. 0.1–0.5 wt.%) were also defective. This could be attributed to the excessively high supply of carbon. Under such conditions, the extreme carbons will dissolve continually into the melted catalysts and then make the catalyst inactive due to the fast growth of the graphitic sheets [24]. As a result, the formation of SWCNTs decreases, while that of carbon nanoparticles increases, resulting in a low density and also a low purity of SWCNTs.

3.5. Effect of the carrier gas flow rate

Normally, in a floating catalyst CVD, carrier gases such as argon and hydrogen are utilized to feed catalyst sources into a reactor. However, little research [13] has been done on the effect of the flow rate of carrier gas on the formation of SWCNTs. In this section, the influence of Ar flow rate in the range of 0.5–3.0 L/min on the formation of SWCNTs was investigated.

We found that CNTs could be formed within an optimal flow range. SEM results (not showed here) showed that the length of CNTs tended to reduce as increasing the flow rate. Under a high flow rate above 2.5 L/min, only iron particles formed. This could be due to the effect of substrate cooling and/or the short residence time of the catalyst. This result is consistent with an experimental result based on the decomposition of ferrocene in CO atmospheric [21]. However, an optimal flow range for CNT formation in our experiment was wider (0.5–2.5 L/min). Additionally, the color of the obtained films changed from black to light black when the flow rate was increased, due to the amount of material deposited.

Fig. 7(a) and (b) shows the Raman spectra of CNT films deposited as a function of argon flow rate (0.5–2.0 L/min). The deposition conditions were 700 °C, 1.0 wt.% ferrocene/ethanol ratio and 15 min. The weaker intensity of peaks (RBM, D- and G-

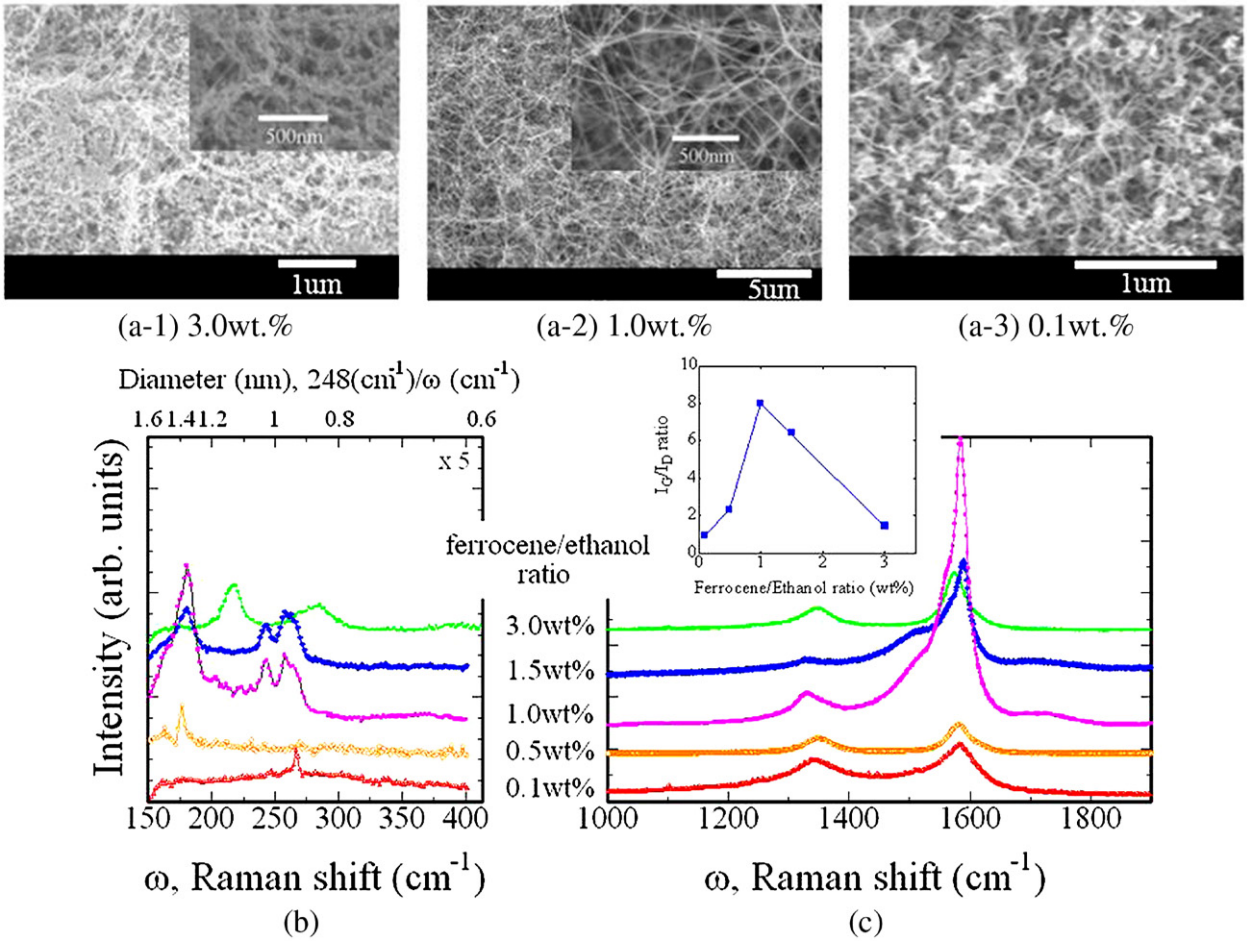

Fig. 6. (a) SEM images of the samples deposited with different ferrocene/ethanol ratios; (a-1) 3.0 wt.%, (a-2) 1.0 wt.% and (a-3) 0.1 wt.%. (b and c) Raman spectra in low and high-frequency regions of CNT films deposited as a function of ferrocene/ethanol ratio. Inset in (c) shows the calculated I_G/I_D values. Growth parameters; furnace temperature: 700 °C, Ar flow rate: 1.0 L/min, position: $z=10$ cm, 15 min.

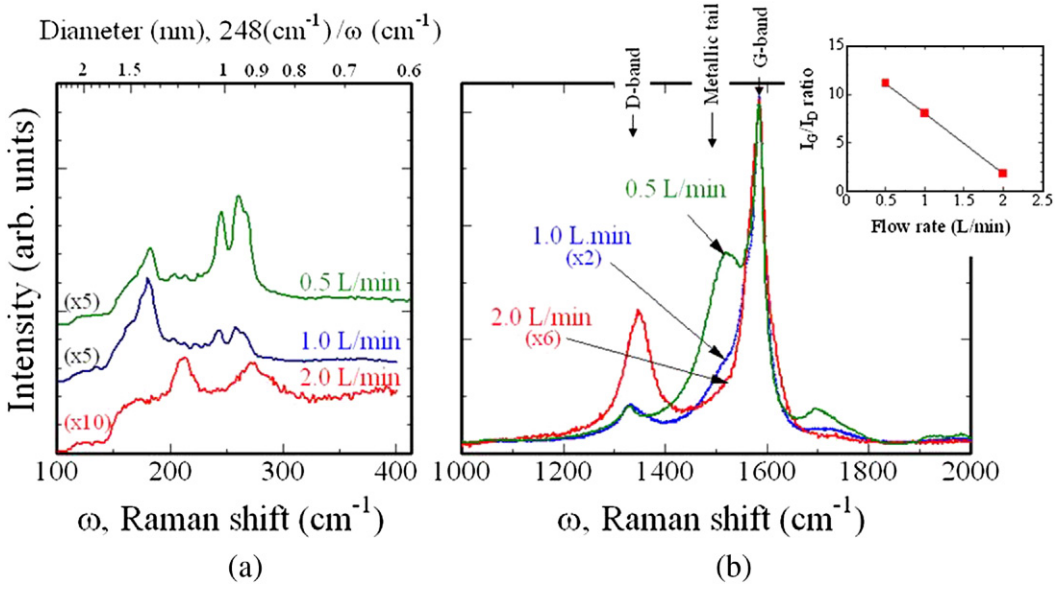

Fig. 7. Raman spectra in (a) low-frequency region and (b) high-frequency region of CNT films deposited at different flow rates. Inset in (b) shows the corresponding I_G/I_D values. Growth parameters; furnace temperature: 700 °C, ferrocene/ethanol ratio: 1.0 wt.%, position: $z=10$ cm, 15 min.

bands) in the high flow rate samples than in the low flow rate samples could be related to a smaller density of nanotubes in the high flow rate samples. When the flow rate was increased, the RBM peaks shifted slightly towards higher wavenumbers, indicating that the diameter of CNTs became smaller. This result is in agreement with earlier findings [13]. This may be explained that the high flow rate of carrier gas prevents the aggregation of catalyst, due to the decrease in residence time of catalyst in the reactor [25]. These effects lead to the smaller catalyst particle size [21], and subsequently, the narrower CNT diameter.

Furthermore, the split of G-band peaks was clearly observed in the obtained CNT films, as illustrated in Fig. 7(b). The narrow and symmetric peak (Lorentzian lineshape) measured at 1584 cm^{-1} can be associated with the semiconducting SWCNTs, while the board and asymmetric peak (Breit–Wigner–Fano lineshape) centered around 1530 cm^{-1} can be assigned to the metallic SWCNTs [26]. These spectral features of the G-band suggest the existence of both semiconducting and metallic tubes in the as-grown materials [7,16,26]. From Fig. 7(b), we found an interesting thing that the intensity of metallic tail decreased with increasing the argon flow rate, resulting in a reduction in mixture ratio of metallic tubes in the films. This result indicates that the flow rate of carrier gas may be an effective parameter to control the mixture ratio between the metallic and semiconducting tubes

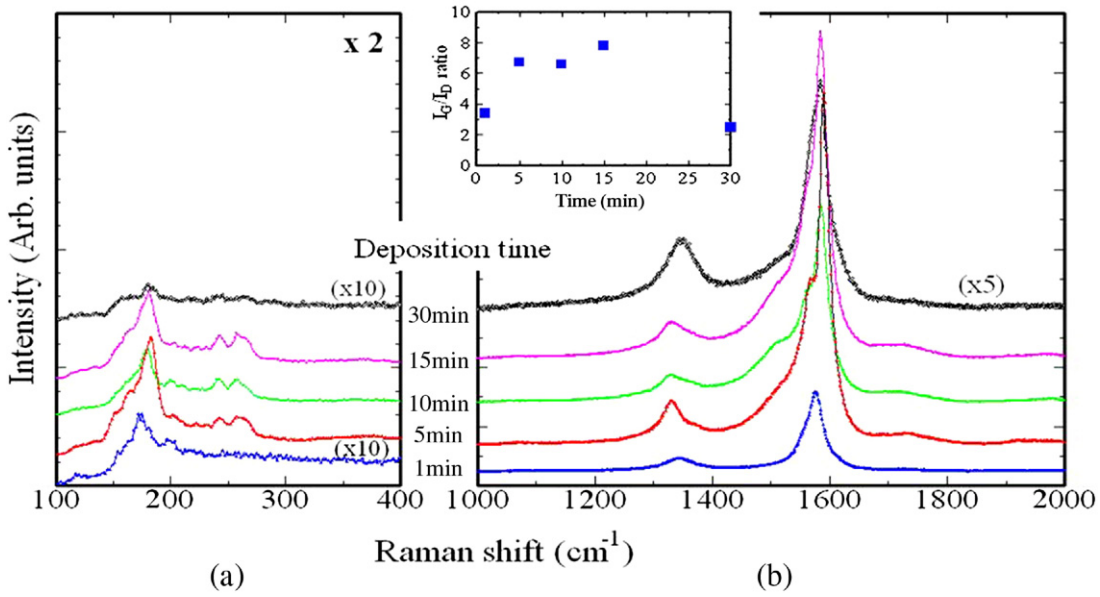

Fig. 8. Raman spectra in (a) low-frequency region and (b) high-frequency region of CNT films deposited as a function of deposition time. Inset in (b) shows the I_G/I_D value. Growth parameters; furnace temperature: 700 °C, ferrocene/ethanol ratio: 1.0 wt.%, Ar flow rate: 1.0 L/min, position: $z=10$ cm.

of the resulting material. However, the I_G/I_D value decreased when the flow rate was increased, as shown in the inset in Fig. 7 (b). This could be due to the incomplete decomposition of vapor sources, as a result of the reduction of residence time of gases in the reactor. To realize the producing of high-crystallinity semiconducting SWCNT, a future investigation is needed.

3.6. Effect of deposition time

Fig. 8 shows the Raman spectra of CNT films deposited as a function of deposition time. The deposition time was varied between 1 min and 30 min. The furnace temperature, ferrocene/ethanol ratio and Ar flow rate were set to 700 °C, 1.0 wt.% and 1.0 L/min respectively. To avoid the residual carbon in the reactor, the oxidation process by heating a quartz tube in air at a high temperature, were employed before each experiment.

SEM and Raman analysis revealed that the formation of narrow-diameter CNTs occurred even at a short deposition time of 1 min. As can be seen from Fig. 8(a), the position of RBM peaks did not change with the deposition time, indicating no change in the diameter of SWCNTs. Examination of the I_G/I_D value in Fig. 8(b) revealed that the samples deposited for 5–15 min resulted in the highest crystallinity index, while those deposited for longer time showed the low value. The observed decrease in crystallinity as the reaction time increased was correlated with the condensation of the ferrocene/ethanol droplet to the liquid phase, which could be observed at the entrance of quartz reactor for a long deposition time (>20 min). At this point, recently we have found that the worming of the connecting pipes between the mist source and quartz reactor may considerably contribute to the continuous formation of CNTs. More information will be presented in the following paper.

4. Conclusions

The floating catalyst CVD under atmospheric pressure using atomized droplets of ferrocene–ethanol mist was successfully used to deposit web-like films consisting of single-walled carbon nanotube (SWCNTs). The experimental results indicated that the CVD parameters must be selected carefully to deposit uniform and high-quality SWCNT films. By varying the furnace temperature, the formation of SWCNTs could be observed when the temperature was higher than 650 °C. In contrast to the hot region at the center of furnace, the worm region outside the furnace was found to be a suitable position toward SWCNTs. This advantage of low substrate temperature may be suitable for the fabrication of CNT-based sensors [27]. The furnace temperature and the flow rate of carrier gas were found to determine the diameter and crystallinity of CNTs. The ferrocene concentration in ethanol strongly influenced the amount of undesirable impurity particles in the material and also the crystallinity of CNTs. There was no significant relation between the deposition time and the diameter of CNTs. Interestingly, the intensity of metallic tail in D-band was found to decrease as the argon flow rate increased, showing a possibility of the production of semiconducting SWCNTs. However, to realize the producing of high-crystallinity semiconducting SWCNT, a future investigation is needed.

Acknowledgements

This work was supported by the National Electronics and Computer Technology Center (Nectec) under contact no. NT-B-22-E3-23-47-09 and the faculty of engineering, King Mongkut's Institute of Technology Ladkrabang (KMITL). S. Chaisitsak thanks P. Srichompol, P. Chiwsitthiprapai and N. Kasikornrungroj (NEMD Lab. colleagues) for their technical assistance and the Electronics Research Center of KMITL for some equipment.

References

[1] S. Ijima, Nature 354 (1991) 56.
[2] M.S. Dresselhaus, G. Dresselhaus, P. Avouris, Carbon Nanotubes: Synthesis, Structure, Properties, And Applications, Springer, 2001.
[3] S. Maruyama, R. Kojima, R. Miyauchi, S. Chiashi, M. Kohno, Chem. Phys. Lett. 360 (2002) 229.
[4] A. Okamoto, H. Shinohara, Carbon 43 (2005) 429.
[5] H. Kataura, Y. Maniwa, T. Kodama, K. Kikuchi, K. Hirahara, K. Suenaga, S. Iijima, S. Suzuki, Y. Achiba, W. Kratschmer, Synth. Met. 121 (2001) 1195.
[6] Y. Li, I.A. Kinloch, A.H. Windle, Science 304 (2004) 276.
[7] F. Lupo, J.A. Rodriguez-Manzo, A. Zamudio, A.L. Elias, Y.A. Kim, T. Hayashi, H. Muramatsu, R. Kamalakaran, H. Terrones, M. Endo, M. Ruhle, M. Terrones, Chem. Phys. Lett. 410 (2005) 384.
[8] B.H. Kim, K. Ueda, O. Sakurai, N. Mizutani, J. Ceram. Soc. Jpn. 100 (1992) 246.
[9] A. Aguilar-Elguezabal, W. Antunez, G. Alonso, F.P. Delgado, F. Espinosa, M. Miki-Yoshida, Diamond Relat. Mater. 15 (2006) 1329.
[10] L.F. Su, J.N. Wang, F. Yu, Z.M. Sheng, H. Chang, C. Pak, Chem. Phys. Lett. 420 (2006) 421.
[11] M. Pinault, M.M. Hermite, C. Reynaud, V. Pichot, P. Launois, D. Ballutaud, Carbon 43 (2005) 2968.
[12] C. Singh, M.S.P. Shaffer, A.H. Windle, Carbon 41 (2003) 359.
[13] A. Barreiro, C. Kramberger, M.H. Rummeli, A. Gruneis, D. Grimm, S. Hampel, T. Gemming, B. Buchner, A. Bachtold, T. Pichler, Carbon 45 (2007) 55.
[14] R.J. Lang, J. Acoust. Soc. Am. 43 (1962) 6.
[15] H. Hou, A.K. Schaper, F. Weller, A. Greiner, Chem. Mater. 14 (2002) 3990.
[16] M.S. Dresselhaus, G. Dresselhaus, R. Saito, A. Jorio, Phys. Rep. 409 (2005) 47.
[17] M. Endo, Y.A. Kim, Y. Fukai, T. Hayashi, M. Terrones, H. Terrones, M.S. Dresselhaus, Appl. Phys. Lett. 79 (2001) 1531.
[18] M. Kumar, Y. Ando, Diamond Relat. Mater. 12 (2003) 1845.
[19] H. Zhang, E. Liang, P. Ding, M. Chao, Physica, B 337 (2003) 10.
[20] H.M. Cheng, F. Li, G. Su, H.Y. Pan, L.L. He, X. Sun, M.S. Dresselhaus, Appl. Phys. Lett. 72 (1998) 3282.
[21] A. Moisala, A.G. Nasibulin, D.P. Brown, H. Jiang, L. Khriachtchev, E.I. Kauppinen, Chem. Eng. Sci. 61 (2006) 4393.
[22] K. Kuwana, K. Saito, Carbon 43 (2005) 2088.
[23] S. Inoue, Y. Kikuchi, Chem. Phys. Lett. 410 (2005) 209.
[24] H. Kanzaw, A. Ding, Phys. Rev., B 60 (1990) 11180.
[25] M. Endo, Y.A. Kim, T. Takeda, S.H. Hong, T. Matusita, T. Hayashi, M.S. Dresselhaus, Carbon 39 (2001) 2003.
[26] H. Kataura, Y. Kumazawa, Y. Maniwa, I. Umezu, S. Suzuki, Y. Ohtsuka, Y. Achiba, Synth. Met. 103 (1999) 2555.
[27] S. Chaisitsak, J. Nukeaw, A. Tuantranont, The 5th IEEE Conference on Sensor 2006, Korea, 2006, p. 297.